Hindawi
International Transactions on Electrical Energy Systems
Volume 2022, Article ID 5771094, 21 pages
https://doi.org/10.1155/2022/5771094

Research Article

An Optimization Method of Active Distribution Network Considering Time Variations in Load and Renewable Distributed Generation

Juan Wen, Xing Qu, Siyu Lin, Lin Ding, and Lin Jiang

College of electrical engineering, University of South China, Hengyang, 421000, China

Correspondence should be addressed to Juan Wen; 55wenjuan@163.com

Received 15 July 2022; Revised 26 October 2022; Accepted 16 November 2022; Published 7 December 2022

Academic Editor: Santi A. Rizzo

Network optimization is one of an effective ways to enhance the performance of an active distribution network (ADN). Aiming to improve the operation and power quality of the ADN considering time variations in load and renewable distributed generation (RDG) power, a multi-time period optimization model and its dynamic solution method are proposed. Considering the real time load demand and power generation variation of RDG versus input parameters like wind speed and solar irradiance, the time variation models of load and RDG power output are developed. The minimum power loss and maximum absorption of RDG power are served as the optimization indexes to construct the dynamic muti-time period optimization model. A hybrid particle swarm optimization (HPSO) algorithm is presented based on integer coding and random coding technique, which can find the most satisfactory solutions for the proposed dynamic model. Considering the time variation of load and RDG power of ADN, the optimal network structure and RDG allocation scheme at any time interval are determined by analyzing the obtained solutions. Additionally, two ADNs with time variation in load and RDG are tested to verify the effectiveness and superiority of the proposed dynamic optimization model and HPSO algorithm. The simulation results show that the proposed method can improve the operation performance and RDG optimal utilization of the ADNs through muti-time period dynamic optimization.

1. Introduction

The application of RDG is a topic that attracts a great deal of interest in the electric power industry because it can reduce the dependency on fossil fuels and environmental pollution [1]. The integration of RDG in the ADN is growing rapidly in discussions about the future of distribution systems with the increased demand for electrical power and the requirement of environmental conservation [2, 3]. The share of RDG in primary energy supply would rise from 14% in 2015 to 63% in 2050 [4]. Recently, wind and solar photovoltaic (PV) RDG technologies are being integrated with ADN because they are easy to install, low operating costs, and mature technology [5, 6]. Taking wind power generation as an example, wind energy would share 15.7% of global electric power consumption by 2020 [6]. The integration of RDG would improve the operation performance and power supply shortage of ADN. Nevertheless, the high-level penetration of RDG brings new challenges affecting the dispatching operations of ADNs [7]. Moreover, The output power of RDGs exhibits fluctuations and intermittency because it depends on input parameters, which places high requirements on the adaptability and control of ADNs. For example, the loss of a single 400-kilovolt transmission line in the India blackout causes sizeable voltage deviations and around 300 million customers without power [8]. Various control actions have been performed to tackle the uncertainties in ADNs, such as network optimization, controllable loads, etc., [9, 10].

Network optimization is a critical issue in distribution systems dispatching management. One effective optimization way is network reconfiguration which is implemented on ADN in the presence of RDG. The method is the process of finding the optimal topology to satisfy the operational objective and constraints [11]. There are some operational

problems with the integration of RDG [12], such as economic dispatch, voltage oscillations, and harmonic distortion. Furthermore, operational conditions of ADN will become more severe when the characteristic of time-varying load conditions and the uncontrollability of RDG output power are both considered [7]. The operational conditions of ADN change frequently along with the time-varying characteristics of RDG and load. In the ADN, flexible and effective control measures are required to apply the frequently changing of operational conditions. We aim to analyze a potential network optimization scheme for improving the performance of the ADN.

In [13], Merlin and Back first propose the concept of network optimization which is obtained the optimal topological configuration with the objective of minimum power loss. And then, the objective functions are extended as load balance [14], voltage deviations [15], power quality [16], and so on. The network optimization is defined as an optimization problem which should satisfy ADN operational objectives and constraints. The obtained optimal solutions of the optimization problem is a challenging task because the search space of solutions is typically large. Many intelligent evolutionary approaches are adopted to address the combinatorial problem such as genetic algorithm (GA) [17], improved decomposition based evolutionary algorithm (I-DBEA) [18], particle swarm optimization (PSO) [19], and so on.

The integration of RDG brings many potential benefits to ADNs, such as minimizing power losses, improving voltage profile, enhancing system stability etc [20]. However, the fluctuation of RDG output in the ADN results in node overvoltage swells and reverse power flow of the system. For instance, reference [22] has shown the changes in ADN stability and economic indicators while the RDG sizing and siting are changed. For this reason, researchers have shown interest to obtain an optimal management scheme for RDG in ADNs using network optimization. In [23, 24], the optimization model with the objectives of RDG units sizing and sitting are established which allocates RDG to the optimal places of ADN. In [25], an energy management scheme of dispatchable wind and PV RDG is proposed to balance the power generation and load demand. It is noteworthy that the methods have been subjected to static network optimization theory and ignored the time variations in RDG. The static optimization model for non-variable RDGs cannot demonstrate real-time scenarios and cannot achieve the optimal RDG configuration scheme considering time scheduling of the ADNs.

The RDG output power has strong uncertainty and time-varying because it is mostly influenced by wind speed and solar irradiance [26]. These characteristics bring new challenges to the calculation and evaluation of the ADN network optimization problem [27]. In [28], a forecast model is used to obtain the RDG variable power at future time interval. In [29], a planning model of wind and solar generations considering uncertainty is proposed to obtain an optimal mix scheme and sizing of various RDG in microgrids. However, The mentioned studies have been performed based on non-variable load models and addressed the network optimization during a predetermined time interval.

Considering time scheduling of the load in ADN, reference [30] presents the optimization model of different time horizons with aiming to reduce switching costs. In [31], the optimally allocate RDG units have been investigated in ADN with time-varying load demand. The model considering load demand and RDG is proposed to solve the ADN optimization problem over a 24-hour time horizon [32]. An optimization model based on RDG fuzzy uncertainty is presented to obtain the optimal topology with objectives of power loss reduction and voltage stability improvement [33]. However, the obtained strategy is not suitable for online real-time network optimization due to the load and RDG based on a fixed prediction. In [34], the optimal management scheme of wind RDG in ADN is proposed on the basis of the probabilistic generation assumption. The solution for the optimization model in the presence of time variation in load and wind RDG is not evaluated markedly.

Reference [35, 36] investigates the operation performance of the ADN based on the conditions of load variation and wind RDG penetration level. The obtained results have not been suitable for the ADN with the integration of multi-type RDG simultaneously. In [37, 38], the optimization methods considering multiple types of RDGs and load demand are proposed to improve the operational management of the ADN. However, the obtained solutions have the coordination between the load and RDG. During the process of ADN network optimization, operational and calculation conditions would become complicated with network size, the type and number of RDGs, and the length of the operation horizon. In addition, the above methods did not evaluate the operational indicators of the optimized ADN from the overall perspective.

In an ADN with high penetration of RDGs, applying actual operation data to model time variation and fluctuation behaviours of the RDGs and loads is a practical solution for distribution operations. An ideal optimization model should consider dynamic optimization of network topology, optimal management scheme for RDGs, and satisfying demand in a reliable and stable way considering time variations in RDGs and loads. However, the operational and calculation conditions would become complicated since the characteristic of time variation in load and RDG during the network optimization of ADN. It is obviously that the mathematical methods are very hard to solve this optimization problem. Furthermore, the voltage oscillations and fault currents in the ADN may increase after RDG integration. The mentioned problems would be more severe in the process of optimization considering the time-varying load and RDG conditions. Although a countermeasure is presented to restrict the output power of RDG by installing control devices, it is not benefit to the effective utilization of RDG. Moreover, due to the characteristic of time variation in load and RDG, the optimization problem size is typically large which needs to identify the switch statuses of multiple time steps. Thus, the coordination mechanism between load and RDG is more complicated in the ADN optimization problem

considering time variations feature. To address these challenges, we present the important theories of the network optimization problem for ADN [39]. Based on the theory in [39], a multi-period optimization model and its methods are proposed to obtain suitable optimal operation schemes for real-time ADN systems in this paper. The optimization model allows the topological network to change in each time interval of the optimization cycle. And the model can realize fast adjustment of operation scheme under real-time load and RDG output. Moreover, a dynamic optimization method is proposed to handle the multi-period optimization problem of conflicting objectives to find the optimal solution for each time interval. The key contributions of this paper are as follows:

(1) An ADN network model that is close to the actual situation of the project is established. In the network model, the maximum RDG power in any time interval is determined by combining network optimization, load demand, and RDG model.

(2) A multi-period optimization model for the ADN considering time variations in load and RDG is derived. The model aims to reduce the system power loss and improve RDG utilization by changing real-time topology at any time interval. Moreover, the overall evaluation indices of ADN operation performance are designed for a given optimization cycle.

(3) To balance the optimization objectives, the normalization and weight methods are used to establish a comprehensive objective function. Considering the dynamic characteristic of the optimization process, the normalized based values of the sub-objective functions for k time interval are the optimal value of the previous stage. Then the comprehensive objective function is derived by using the average weight method.

(4) A hybrid particle swarm optimization (HPSO) based on mixed code is used to find the optimal topology and RDG power for every time interval corresponding to conflicting objectives. Since the load demand and RDG power are time-varying, the proposed method is continuous guiding the search for the optimal solution in the next time interval according to the optimal solution of the previous period.

(5) Due to the differences in dimensions and representation between the topology and RDG power, the proposed method uses integer coding based on loop network and random number coding distribution to represent the variables. The globally optimal solution is obtained by simultaneously updating quantum position of mixed variables, which improves the search efficiency of the proposed method.

The rest of this paper is organized as follows: Section II gives the time-varying of load and RDG model. Sections III presents the problem of mathematical formulation. Section IV provides the HPSO method to apply to the network optimization problem. Section V presents simulation results of two ADNs. Finally, section VI outlines conclusions.

2. Load and RDG model

2.1. Load model. In a practical scenario, the load of the ADN changes in real time because it depends on the actual demand of various type loads. Usually, the comprehensive load model of ADN is the sum of the demands of residential, commercial and industrial loads [37]. Fig 1 shows the actual hourly load for residential, commercial and industrial load patterns at a node in the ADN.

For any k time interval, the comprehensive load P_{Li}^k of i node is represented as (1),

$$P_{Li}^k = P_{Ri}^k + P_{Ii}^k + P_{Ci}^k, \tag{1}$$

where P_{Li}^k, P_{Ri}^k, P_{Ii}^k, and $P_{Ci}^k$are comprehensive power load, residential power load, industrial power load, and commercial power load at k time interval.

2.2. RDG model

2.2.1. (1) wind RDG model. Wind RDG output power is often affected by some factors like weather conditions, temperature, and so on. In particular, wind speed is one of the influencing factors on the output power of wind RDG. Based on the statistical data and experience of the operators, the best expression for depicting the distribution of wind speed behavior is Weibull probability density function (PDF) [40]. The output power of wind RDG can be modeled by wind speed variable, in which the Weibull PDF is adopted to describe the distribution characteristics of wind speed. random feature and uncertainty of the wind speed. For k time interval, the actual wind RDG output behavior can be modeled as [39]:

$$P_w^k = \begin{cases} 0 & 0 \le v^k \le v_{in}^k \cup v_{\text{out}}^k \le v^k, \\ P_r^k \dfrac{v^k - v_{in}^k}{v_r^k - v_{in}^k} & v_{in}^k \le v^k \le v_r^k, \\ P_r^k & v_r^k \le v^k \le v_{\text{out}}^k, \end{cases} \tag{2}$$

where, for k time interval, P_r^k is the rated power of wind RDG, P_w^k is the actual wind RDG output power, v^k is average wind speed,v_{in}^k is cut in wind speed, v_{out}^k is cut out wind speed, and v_r^k is rated wind speed.

2.2.2. (2) PV RDG model. The PV RDG output is closely related to the factor of solar irradiance. The appropriate function to characterize solar irradiance is Beta PDF. For k time interval, the obtained solar irradiance function by using Beta PDF is represented as follows [39]:

$$f\left(r^k\right) = \frac{\Gamma(\alpha+\beta)}{\Gamma(\alpha)\Gamma(\beta)} \left(\frac{r^k}{r_{\max}}\right)^{\alpha-1} \left(1 - \frac{r^k}{r_{\max}}\right)^{\beta-1}, \tag{3}$$

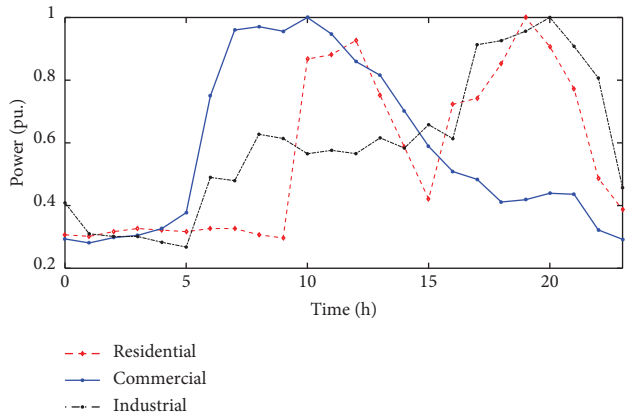

Figure 1: Actual duration curves of three load patterns.

where, for k time interval, $\Gamma(\cdot)$ is the Gamma function, $f(r^k)$ is solar irradiance distribution function, r^k and r_{max} represent actual value and maximum value of solar irradiance, α, β represent the shape variables of Gamma function.

Similarly, the mathematical equation of PV RDG output is formulated as:

$$f\left(P_{Vw}^k\right) = \frac{\Gamma(\alpha+\beta)}{\Gamma(\alpha)\Gamma(\beta)}\left(\frac{P_{Vw}^k}{E_P}\right)^{\alpha-1}\left(1-\frac{P_{Vw}^k}{E_P}\right)^{\beta-1}, \quad (4)$$

where P_{Vw}^k is the actual output of PV RDG at k time interval, E_p is maximum power of PV RDG and its calculation equation is expressed as:

$$E_P = r_{\max} A \eta_{pv}, \quad (5)$$

Where, A and η_{pv} are the total area of PV panels and the efficiency of PV conversion.

For k time interval, assuming that φ is a variable of power angle, the relational expression of active power P_{RDG}^k and reactive power Q_{RDG}^k of RDG models is shown as follows [41].

$$Q_{RDG}^k = P_{RDG}^k \tan\varphi. \quad (6)$$

2.3. Mathematical Formulation

2.3.1. Objective Functions. According to various load demands, the comprehensive load of ADN would randomly decrease or increase in real time. And the output power of RDG changes in real time with the change of wind speed and solar radiation. The ADN network optimization is a dynamic process because of the time-varying features of load and RDG. Therefore, the optimization process in the model will be performed along the time intervals. Considering the engineering actual situation of the ADN, we seek the optimal operational scheme to enhance the operational performance of the ADN system. In this paper, the goal is to find the optimum configurations which have the minimum power losses and maximum RDG utilization simultaneously for all time intervals.

(1) Evaluation index of power loss

The active power loss on the line is an important index to evaluate the system loss. For k time interval, the optimization problem is to find an optimal radial configuration that gives minimum active power loss. It is described as:

$$F_1^k = \min\left(f_1^k\right) = \min\left(\sum_{l=1}^{N_l} z_l^k r_l^k \frac{\left(P_l^k\right)^2+\left(Q_l^k\right)^2}{\left(U_i^k\right)^2}\right), \quad (7)$$

For a given time, the total active power loss $F_{1\text{total}}$ of the ADN is the sum of the power losses of all sub-time intervals.

$$F_{1total} = \sum_{k=1}^{N_H} f_1^k = \sum_{k=1}^{N_H}\sum_{l=1}^{N_l} z_l^k r_l^k \frac{\left(P_l^k\right)^2+\left(Q_l^k\right)^2}{\left(U_i^k\right)^2}, \quad (8)$$

where, for k time interval, f_1^k is the system power loss, l is branch label connecting node i and node j,P_l^k and Q_l^k are the active and reactive power of l branch, r_l^k is the l branch resistance, U_i^k is voltage amplitude at node i, z_l^k is a binary variable. If z_l^k represents the opening switch status, $z_l^k = 1$, otherwise, $z_l^k = 0$. N_l and N_H represent the total number of branches and time sub-intervals.

(2) Evaluation index of RDG utilization

The network operation mode of ADN is dynamic and variable because of time variations in load and RDG power. In the optimization method of ADN, the index of RDG utilization should be considered while improving the power quality and economy. For k time interval, the sub-objective is to find the network configuration of ADN such that it has the maximum capability of RDG integration $F_{2\text{in}}$.

$$F_{2\text{in}}^k = \max\left(f_2^k\right) = \max\left(\sum_{h=1}^{N_G} \delta_h P_{RDGh}^k\right). \quad (9)$$

To maintain consistency with the optimization method, the optimization objective can be transformed into (10).

$$F_2^k = \min\left(\frac{1}{f_2^k}\right) = \min\left(\frac{1}{\sum_{h=1}^{N_G}\delta_h P_{RDGh}^k}\right). \quad (10)$$

RDG utilization ($F_{RDG\%}$) is defined as an estimate of total absorption RDG power by the ADN during a given time.

$$F_{RDG\%} = \left[\frac{\left(\sum_{k=1}^{N_H}\sum_{h=1}^{N_G}\delta_h P_{RDGh}^k\right)}{\left(\sum_{k=1}^{N_H}\sum_{h=1}^{N_G}\delta_i P_{RDGh\max}^k\right)}\right]\times 100\%, \quad (11)$$

where h represents the index label of the RDG, N_G is the number of RDG, δ_h is a binary variable representing the connection status between RDG and network, which takes $\delta_h = 1$ if the RDG is synchronized with the network and $\delta_h = 0$ otherwise. P_{RDGh}^k and $P_{RDGh\max}^k$ are actual output power and maximum output power of h RDG at k time interval, f_2^k is total output power of RDGs at k time interval.

(3) Comprehensive objective function

Due to the difference in the variation range and dimension of parameters, we should be normalized to eliminate the difference of sub-objective functions. For k time interval, the topological structure of ADN optimization is based on the topology of the previous stage. Therefore, the normalized standard value of power loss of k time interval is obtained by combining the topological structure of k-1 time interval and load demand of k time interval. The normalized standard value of RDG output power is the sum of the upper limit RDG power in each period. The normalized standard expression of the sub-objective functions can be expressed as:

$$F_{1nor}^{k} = \sum_{l=1}^{N_l} z_l^{k-1} r_l^{k-1} \frac{\left(P_l^k\right)^2 + \left(Q_l^k\right)^2}{\left(U_i^k\right)^2}. \tag{12}$$

$$F_{2nor}^{k} = \left(\frac{1}{\sum_{h=1}^{N_G} \delta_h P_{RDGh\max}^{k}} \right), \tag{13}$$

Where F_{1nor}^{k} and F_{2nor}^{k} represent the normalized standard values of power loss and RDG output power in k time interval, respectively.

Conflict is certain existed in the objectives of RDG utilization and power loss. For example, the power loss of ADN will be very high if the penetration of RDG reaches a certain value. For coordinating the indices, we assign different significance weight coefficients to the sub-objective functions. Thus, a muti-period comprehensive optimization objective function is formulated by the weight coefficient method. The normalized comprehensive objective function for k time interval is defined as follows:

$$F^{k} = \sigma_1 \frac{F_1^k}{F_{1nor}^k} + \sigma_2 \frac{F_2^k}{F_{2nor}^k} \tag{14}$$

where $\sigma_1 + \sigma_2 = 1$ and $\sigma_1, \sigma_2 \in [0, 1]$.

2.3.2. Constraints. The operating constraints include power flow constraint, voltage constraint, radial topology constraint, Branch apparent power flow constraint, and RDG constraint. These constraints are described in detail in [39], and only relevant expressions are listed here.

$$\begin{cases} P_{si}^k + P_{RDGi}^k - P_{Li}^k = U_i^k \sum_{j=1}^{N} z_l^k U_j^k \left[g_l^k \cos\left(\theta_l^k\right) + b_l^k \sin\left(\theta_l^k\right) \right], \\ Q_{si}^k + Q_{RDGi}^k - Q_{Li}^k = U_i^k \sum_{j=1}^{N} z_l^k U_j^k \left[g_l^k \cos\left(\theta_l^k\right) - b_l^k \sin\left(\theta_l^k\right) \right]. \end{cases} \tag{15}$$

$$U_{i\min}^{k} \le U_i^k \le U_{i\max}^{k}. \tag{16}$$

$$T_g^k \in T_{Gr}. \tag{17}$$

$$S_l^k \le S_{l\max}^k, \tag{18}$$

$$\begin{aligned} &P_{RDGh\min}^{k} \le P_{RDGh}^{k} \le P_{RDGh\max}^{k} \left(h \in N_G\right), \\ &Q_{RDGh\min}^{k} \le Q_{RDGh}^{k} \le Q_{RDGh\max}^{k}. \end{aligned} \tag{19}$$

where, for k time interval, P_{si}^k and Q_{si}^k are the injected active and reactive power of the node i, P_{Li}^k and Q_{Li}^k are the load demand of node i, P_{RDGi}^k and Q_{RDGi}^k are the actual RDG output power on node i. g_l^k, b_l^k, θ_l^k are conductance, susceptance, phase angle of branch l. U_i^k and U_j^k are voltage amplitude of node i and j. N is the set of nodes of the ADN. $U_i^k, U_{i\min}^k, U_{i\max}^k$ the real time voltage amplitude, lower limit amplitude and upper limit amplitude of node i at k time interval. T_g^k is the reconfigured network topology at k time interval and T_{Gr} is the set of radial topologies. S_l^k, $S_{l\max}^k$ are apparent power flow and the apparent power limit of branch l at k time interval. P_{RDGh}^k and Q_{RDGh}^k are the actual active and reactive power of i RDG at k time interval, $P_{RDGh\min}^k, Q_{RDGh\min}^k, Ph_{RDGh\max}^k, Q_{RDGh\max}^k$ are the minimum and maximum output power of RDGs for k time interval.

3. Methodology

The power flow in ADN is changing frequently with the time variations of load demand and RDG outputs. This paper focuses on the multi-period optimization model which the studied time cycle divides into several sub-time intervals. Several requirements need to be considered in dealing with the multi-period optimization problem combining RDG integration, load demand and network topology. And the HPSO method is chosen to solve the coordination optimization problem.

HPSO is a meta-heuristic optimization model that mimics the swarm characteristics of the foraging behaviour of bird flocks based on the traditional PSO algorithm [42]. The movement of each particle has a random speed that

determines the direction and distance of its flight. Based on the speed update rule and location update rule, the algorithm brings about local search and global information exchange during the optimization process. In the traditional PSO, the speed and position of each particle are described as random vectors. In our study, a particle is composed of the opened switch number of a possible radial network configuration and potential RDG power. The opened switch number is usually expressed as an integer code, and the RDG power can be a random code. Moreover, the method should be efficient to address the multi-time period optimization problem. The concepts are considered within the traditional PSO to develop an HPSO method discovering a set of solutions of multi-time period and multi-objective optimization model. The procedure of HPSO is shown in Fig 2. Based on the [39], the detailed implementation process of the HPSO is as follows.

Step 1. Calculating the output power of RDGs for each time interval. The maximum outputs of RDGs for sub-time intervals are obtained by measuring the real-time input parameters of RDG such as wind speed and solar irradiance. The PSO is used to determine the base values P_r and E_p of wind and PV RDGs output power based on the peak load point. We calculate time sequence RDG outputs based on wind and PV RDG models.

Step 2. Inputting the parameters like topology structure, RDG type and location, time sequence RDG outputs and load data, and so on.

Step 3. Designing the multi-period optimization model for a given time. The problem aims to find the best solution that satisfies the requirements of power loss and RDG utilization fixed by distribution manager. For k time interval, the integration RDG number and type are not fixed. For example, there may be no PV RDG power since the solar irradiance is 0. Therefore, the type and number of RDGs connected to ADN for k time interval rely on the real time input parameters of RDG. After that, the multi-time period optimization model is designed as equations (7)-(19).

Step 4. Initializing the population. In the proposed HPSO method, the population is composed of a set of random particles. For k time interval, the best solution to the optimization problem is a particle in the population. A particle is defined as a vector $X_d = [\, x_1 \;\; x_2 \;\; \dots \;\; x_d \,]$ which contains the radial topology and RDG power. The network topology is usually represented by the opened switches in loops that label the integer coded. And the RDG output power is generated randomly. Given an ADN with n loops and N_G RDGs, a random population is represented as equation (20).

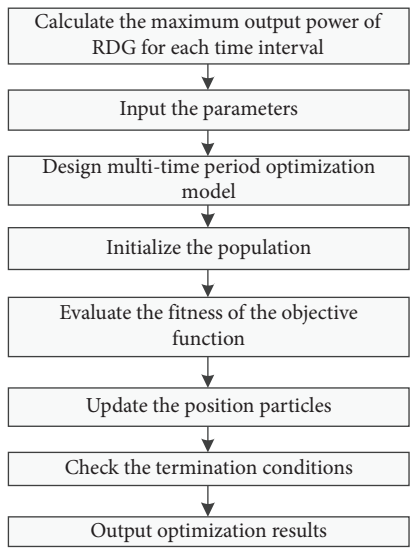

Figure 2: The procedure of HPSO.

$$X_d = \begin{bmatrix} \overbrace{x_{1.1} \;\; x_{1.2} \;\; \cdots \;\; x_{1.n}}^{\text{Swiches lable}} & \overbrace{x_{1.n+1} \;\; \cdots \;\; x_{1.n+N_G}}^{RDG \text{ power}} \\ x_{2.1} \;\; x_{2.2} \;\; \cdots \;\; x_{2.n} & x_{2.n+1} \;\; \cdots \;\; x_{2.n+N_G} \\ \vdots \;\; \vdots \;\; \cdots \;\; \vdots & \vdots \;\; \cdots \;\; \vdots \\ x_{nop.1} \;\; x_{nop.2} \;\; \cdots \;\; x_{nop.n} & x_{nop.n+1} \;\; \cdots \;\; x_{nop.n+N_G} \end{bmatrix}, \tag{20}$$

Step 5. Evaluating the fitness of the comprehensive objective functions. In the proposed method, a forward-backward sweep based load flow method is used to calculate the operation indices of the ADN. The weight coefficient of the objective functions is $\sigma_1 = \sigma_2 = 0.5$. According to equation (14), the objective function values of each particle for k time interval are calculated to identify the best and worst solutions in the entire population. Assuming that the current and global best position of a D-dimensional particle are $p_{md}^k = [\, p_{m1}^k \;\; p_{m2}^k \;\; \dots \;\; p_{mD}^k \,]$ and $p_{gd}^k = [\, p_{g1}^k \;\; p_{g2}^k \;\; \dots \;\; p_{gD}^k \,]$. For t iteration, we obtain the average and optimal best position of M particles in a population are represented as $mbest^k(t)$ and $p_{md}^k(t)$.

$$\begin{aligned} m\text{best}^k(t) &= \frac{1}{M} \sum_{m=1}^{M} p_{md}^k(t), \\ p_{md}^k(t) &= \varphi p_{md}^k(t) + (1-\varphi) p_{gd}^k(t) \, (\varphi \in [0,1]). \end{aligned} \tag{21}$$

Step 6. Updating the position particles satisfying all the operating constraints. For k time interval, the updated position of topology particle $ix_{mdn}^k(t+1)$ and RDG power particle i position $x_{idN_G}^k(t+1)$ after t iteration are obtained.

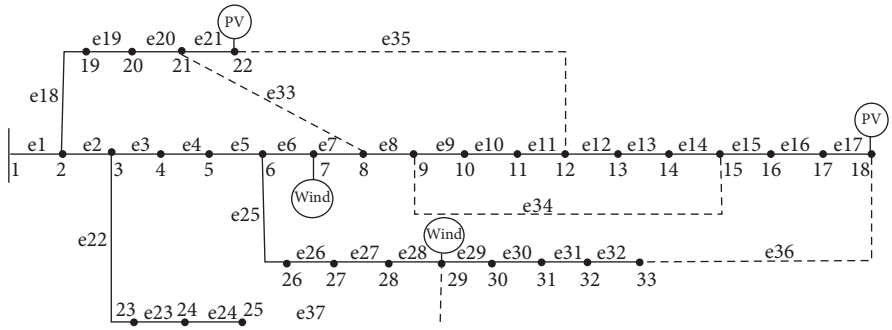

Figure 3: The 33-bus ADN.

$$\begin{cases} x_{mdn}^{k}(t+1) = P_{md}^{k}(t) \pm \lambda^{k} * \left| m\text{best}^{k}(t) - x_{mdn}^{k}(t) \right| * \ln\left(\frac{1}{u}\right) \\ x_{mdN_G}^{k}(t+1) = \text{round}\left(P_{md}^{k}(t) \pm \lambda^{k} * \left| m\text{best}^{k}(t) - x_{mdN_G}^{k}(t) \right| * \ln\left(\frac{1}{u}\right) \right) \end{cases}, \tag{22}$$

$$\lambda_{\max}^{k} = \frac{\left(t_{\max}^{k} - t^{k}\right) \times \beta_{\max}^{k}}{t_{\max}^{k}}.$$

where, for k time interval, λ^k and $\lambda_{\max}^k$ are the current value and upper limit of control coefficient of and convergence speed, u is the uniformly distributed random number, $t_{\max}^k$ is the maximum number iterations

Step 7. Setting t^k=t^k+1 and updating the particle positions p_{md}^k and p_{gd}^k.

Step 8. Checking the termination conditions. The optimization process will be continued until the current iteration is less than equal to the maximum iteration number. The algorithm repeat steps (4)-(7) until these termination conditions are satisfied.

Step 9. Checking the optimization completion for all time intervals N_H. The algorithm repeats steps(2)–(8) until $k \geq N_H$ is satisfied.

Step 10. Output the best optimal results of all time intervals.

4. Case Study And Results

4.1. 33-bus ADN. The multi-time period model and proposed optimization method is tested on an ADN, presented in Fig 3. The system has five loops which the tie-branches are e34-e37. The line impedances can be found in [43]. From Fig 3, the wind and PV RDGs are installed on the corresponding nodes. The voltage fluctuation range is 0.90-1.05 p.u. The comprehensive objective function is shown in (9) which the weight values are set σ_1=σ_2=0.5.

The real-time load of one day is considered an optimization cycle. Based on the load and RDG models, Fig 4 show the actual hourly load demand and output power of RDGs in a certain area.

4.1.1. Benefits of combining network optimization and RDG integration. To analyze the operation performance of ADN after RDG integration and network optimization, three cases are simulated to utilize the proposed method at peak load point.

Case 1. Initial system without RDGs and network optimization.

Case 2. Solving the optimal problem of RDG utilization maximization and power loss minimization without network optimization.

Case 3. Solving the problem of RDG utilization maximization and power loss minimization with network optimization.

In Fig 4, the peak load point of actual hourly load demand is 7.4406MW+4.5314MVar at 19:00. The obtained results of the cases are presented in Table 1.

In case 2, the RDG is optimally integrated utilization without network optimization, providing an 80.2% reduction of system power loss (P_{loss}). However, the P_{loss} is reduced by 89.53% in case 3. Moreover, the absorption RDG power (P_{RDG}) by the system has improved to 6.1836MW after optimization. The combination of network optimization and RDG integration is effective in reducing the system power loss of the ADN.

Fig 5 shows the hourly voltage profiles of all the cases. The voltage amplitude is improved when combining network optimization with RDG integration than when

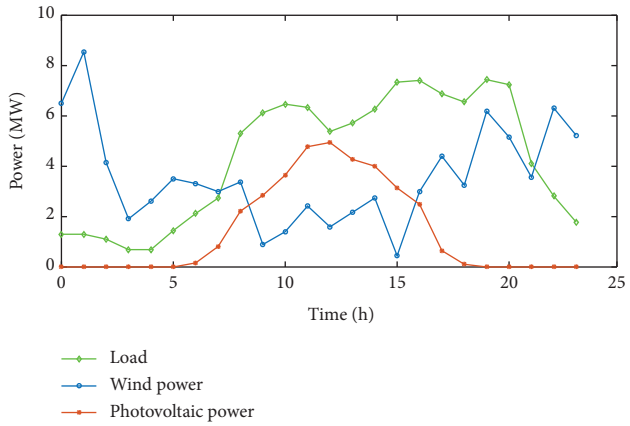

Figure 4: Hourly load demand and RDG power.

Table 1: Benefits of combining network optimization and RDG integration.

Cases	Open switches	P_{loss}/kW	P_{RDG}/MW	$V_{min}/p.u.$
1	e33-e37	954.8644	0	0.8104
2	e33-e37	189.0362	5.9423	0.9494
3	e33, e3, e17, e35, e13	99.9680	6.1836	0.9734

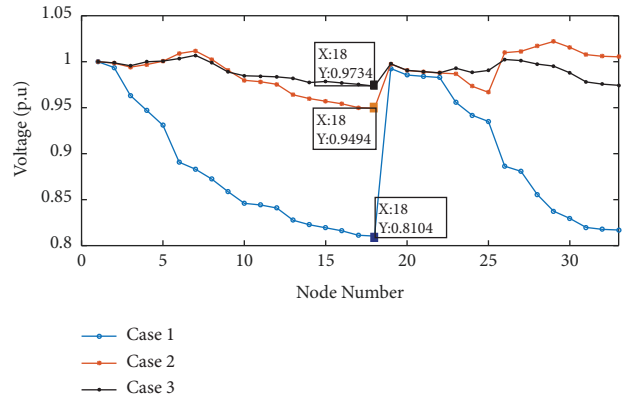

Figure 5: The voltage profile for cases.

integrating RDG only and base system. The minimum voltage (V_{min}) amplitude of case 3 has increased to 0.9734p.u., which is above 0.9494p.u. of case 2 and 0.8104 p.u. of case 1. The results show that system efficiency in the optimization problem with adding the RDG is better than the base system and has resulted in more power loss reduction, more voltage profile change, and more RDG power utilization. The use of RDG along with network optimization leads to better operation conditions of the ADN due to the injection of RDG power.

To justify the superiority of the proposed method, the optimization problem in case 3 is also solved by the conventional algorithms, GA method [43] and moth-flame optimization (MFO) [44]. the obtained simulation results are compared with those obtained by the conventional methods. The methods are based on initial conditions and similar assumptions. Table 2 and Fig 6 illustrate the detailed comparison results.

Table 2: Comparison with last optimization methods.

Items	Open switches	P_{loss}/kW	P_{RDG}/MW	$V_{min}/p.u.$
Proposed method	e33, e3, e17, e35, e13	99.9680	6.1836	0.9734
GA [43]	e33, e28, e17, e35, e13	101.3932	6.1836	0.9662
MFO [44]	e33, e3, e17, e35, e13	99.9680	6.1836	0.9734

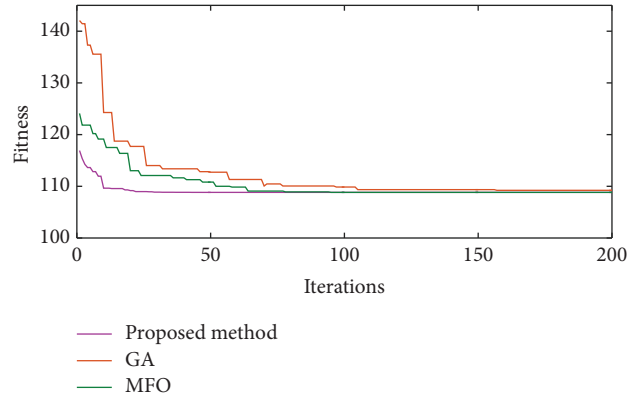

Fig 6: The convergence curve of the IEEE33 bus system.

The proposed method presents a superior performance to the GA and MFO. The proposed method provides an optimal solution with 99.9680kW of system power loss which is less than 101.3932kW in GA algorithm. According to Fig 6, the proposed method could achieve optimal solution faster than other methods, i. e., 47 iterations against 95 in MFO, 47 iterations compared to 157 in GA. Consequently, the proposed method is an effective way for addressing ADN network optimization due to its high convergence ability and accuracy.

4.1.2. Experiment considering time variations in RDG and load. The proposed model and method is used to address the optimization problem of ADN considering the time variations in RDG and load. The hourly data in RDG and load of an average day as an example of study are illustrated in Fig 4. In the 33-bus ADN, four cases are adopted to investigate the effect of time-varying characteristics on network optimization indicators.

Case 4. Load variation is considered without network optimization and RDG.

Case 5. Load variation and network optimization simulation are considered.

Case 6. Time variations in load and RDG are considered without network optimization.

Case 7. Simultaneous hourly network optimization and time variations in load and RDG are studied.

Table 3: The simulation results for cases 4 and 5.

Hour	Case 4			Case 5		
	P_{loss}/kW	$V_{min}/p.u.$	Open switches	P_{loss}/kW	$V_{min}/p.u.$	Open switches
0	22.7169	0.9708		15.4203	0.9800	
1	22.7168	0.9708		15.4203	0.9800	
2	16.3075	0.9746		10.4509	0.9836	e7, e14, e9, e32, e28
3	6.0509	0.9849		4.0918	0.9900	
4	6.0507	0.9849		4.0918	0.9900	
5	26.4839	0.9678		18.6209	0.9774	
6	59.2882	0.9521		41.4271	0.9675	e7, e14, e9, e32, e37
7	102.6528	0.9381		71.6523	0.9557	
8	454.6853	0.8711		299.2572	0.9111	
9	634.7827	0.8465		406.9587	0.8958	e7, e14, e9, e32, e28
10	707.9717	0.8399		458.5657	0.8907	
11	667.9735	0.8449	e33, e34, e35, e36, e37	434.8238	0.8943	
12	450.9375	0.8707		303.2061	0.9095	e7, e14, e9, e32, e37
13	524.2916	0.8622		353.2866	0.9055	
14	655.2344	0.8467		429.3050	0.8945	e7, e14, e9, e32, e28
15	957.7037	0.8154		617.2244	0.8735	
16	972.4477	0.8126		631.8764	0.8646	
17	800.6986	0.8283		523.4494	0.8786	
18	704.0766	0.8373		460.8127	0.8870	e7, e14, e9, e32, e37
19	954.8644	0.8104		612.0081	0.8692	
20	892.3920	0.8166		574.1248	0.8726	
21	245.2501	0.9043		164.6489	0.9364	e7, e14, e9, e32, e28
22	107.0733	0.9359		74.2170	0.9554	e7, e14, e9, e32, e37
23	42.5950	0.9603		29.0150	0.9729	e7, e14, e9, e32, e28

Table 4: the simulation results for cases 6 and 7.

Hour	Case 6				Case 7			
	P_{loss}/kW	V_{min}/pu	P_{RDG}/MW	Open switches	P_{loss}/kW	V_{min}/pu	P_{RDG}/MW	Open switches
0	8.1067	0.9975	1.4218		6.0394	1.0000	1.6812	e18, e26, e15, e35, e13
1	8.1067	0.9975	1.4217		6.0394	1.0000	1.6812	e18, e26, e15, e35, e13
2	5.8469	0.9980	1.2532		4.8468	1.0000	1.4586	e18, e26, e15, e35, e13
3	3.2958	0.9989	0.8466		2.5442	1.0000	0.9858	e18, e26, e15, e35, e13
4	3.2958	0.9962	0.8466		2.5442	1.0000	0.9858	e18, e26, e15, e35, e13
5	15.4035	0.9926	1.5047		14.5019	1.0000	1.7885	e18, e26, e15, e35, e13
6	16.5998	0.9902	2.1212		10.6640	1.0000	2.5000	e18, e26, e15, e35, e13
7	20.7617	0.9791	2.8600		11.7804	1.0000	3.1844	e33, e26, e34, e11, e13
8	67.9496	0.9094	5.1583		32.0832	0.9961	5.5973	e33, e27, e34, e10, e14
9	260.6859	0.9250	3.7394		93.8267	0.9617	3.7394	e20, e28, e7, e9, e14
10	255.5533	0.9539	4.9059		76.6267	0.9785	5.0553	e19, e5, e34, e8, e14
11	145.1387	0.9539	5.2497		63.2703	0.9912	6.3646	e7, e28, e8, e10, e14
12	135.4337	0.9603	4.2558	e33, e34, e35, e36, e37	57.9087	0.9898	5.2516	e3, e28, e8, e9, e13
13	123.2461	0.9625	4.7329		56.2066	0.9912	5.7489	e7, e28, e8, e9, e14
14	126.8513	0.9373	5.3648		60.6288	0.9923	6.4603	e7, e28, e8, e10, e14
15	559.0125	0.8513	1.5438		194.9442	0.9463	3.5852	e6, e37, e15, e8, e 14
16	174.5450	0.9471	5.4858		80.6216	0.9706	5.4860	e20, e5, e15, e10, e 14
17	121.4635	0.9643	5.0480		72.5454	0.9706	5.0480	e33, e4, e17, e11, e14
18	165.7809	0.9210	3.3588		126.0127	0.9492	3.3588	e33, e28, e32, e10, e14
19	194.7916	0.9516	6.0711		99.9680	0.9734	6.1836	e33, e3, e17, e35, e13
20	166.3880	0.9382	5.1636		97.5013	0.9628	5.1636	e33, e4, e17, e11, e13
21	54.0669	0.9768	3.4541		28.3297	0.9859	3.5698	e33, e28, e17, e35, e13
22	30.2893	0.9908	2.6554		20.0171	0.9959	3.2057	e18, e26, e15, e35, e13
23	13.1778	0.9958	1.8297		9.5739	0.9994	2.1778	e18, e26, e15, e35, e13

Using the proposed model and method, we obtained the selected open switches and RDG utilization for a given time certain. Tables 3 and 4 present the simulation results and optimal solutions for each time interval for the cases. In each time interval, the open switches, P_{loss}, V_{min}, and absorbed RDGs power are presented corresponding to each time interval for cases.

In cases 4 and 5, the simulation is carried out in the system with time variation of load demand. Table 3 lists the results of active power loss, minimum node voltage, and

open switches before and after optimization (case 4 and case 5). As seen in Table 3, the optimal solutions with opening switches e7, e14, e9, e32, and e28 are consistent at time intervals 0~4th, 8~11th, 13~15th, 21th, and 23th. The opened switches in other time intervals are e7, e14, e9, e32, and e37 after optimization. The active power loss for each time interval reduces after optimization, i.e, 41.4271kW against 59.2882kW at 6:00, 458.5657kW compared to 707.9717kW at 10:00, 458.6379kW instead of 631.8764kW at 16:00, and so on. Further, it is noted that the minimum node voltage for each interval has increased in case 5 compared in case 4. For example, The percentage improvement in minimum node voltage value after optimization is 1.67%, 5.08%, and 6.40% at 6:00, 10:00, and 16:00, respectively. Fig 7 gives the total power loss and minimum voltage profile in a day of the cases. From Fig 7, the total daily power loss in case 4 is 10.0352MW. The daily total power loss after optimization has been reduced by 34.69%. The minimum voltage amplitude in a day improves to 0.8646p.u. in case 5, which implies an improvement of 6.69% compared to case 4. The results illustrate network optimization can effectively improve the system operation level. However, the daily minimum voltage amplitude 0.8646p.u. in case 5 is lower than the voltage limit of 0.90p.u. It is not conducive to the long-term stable operation of the active distribution system. The way of integration of RDG is considered to improve operating indices.

To perform the suggested method which requires time variations in RDG and load demand, different load profiles and RDG output power are added to the system at each time interval. Table 4 depicts the variations of the operational indices of the system in cases 6 and 7. It is observed that the optimization effects of cases 6 and 7 are better than those of cases 4 and 5. In cases 6 and 7, the obtained optimal solutions provide the total daily power loss are 2.6758MW and 1.2290MW, respectively. The maximum power loss of the day in case 7 is 194.9442kw at 15:00, which implies a reduction of 762.7595kW, 263.0196kW, and 364.0683kW compared to case 4, case 5, and case 6. From Fig 7, the daily minimum voltage amplitude of case 7 is 0.9463p.u., which is higher than the minimum voltage limit 0.90p.u. It indicates that simultaneous network optimization with time-varying load and RDG can improve the performance of the ADN. Moreover, the day absorption RDG power for case 7 is 90.2614MW, which has increased by 12.42% with case 6. And the RDG utilization (RDG%) has been improved from 67.04% in case 6 to 75.37% in case 7.

Due to space reasons, the operational indices of the ADN at 11:00 and 21:00 are analyzed as examples to describe the operation characteristic at each time interval clearly. Fig 8 shows the power loss of each branch at 11:00 and 21:00. In case 4, the power loss of ADN is relatively large without network optimization and integration of RDGs. In case 5, it is significantly reduced after optimization by changing the topology with opening switch combinations [e7, e14, e9, e32, e28]. The system power loss is reduced by 53.62% at 11:00, and 32.87% at 21:00, respectively. After integrating of RDGs, The system power loss for case 6 is reduced by 78.27% at 11:00, and 77.95% at 21:00, respectively. The benefits of

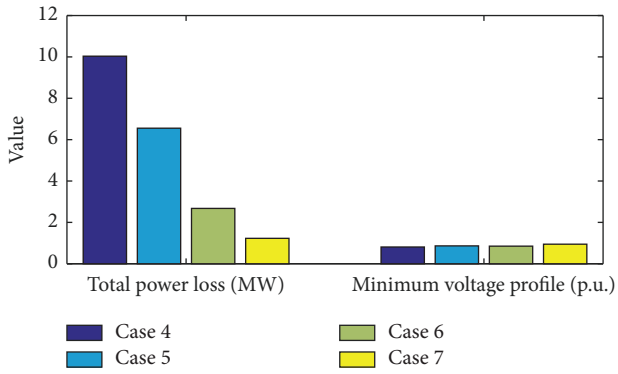

Figure 7: the simulation results for all the cases in a day.

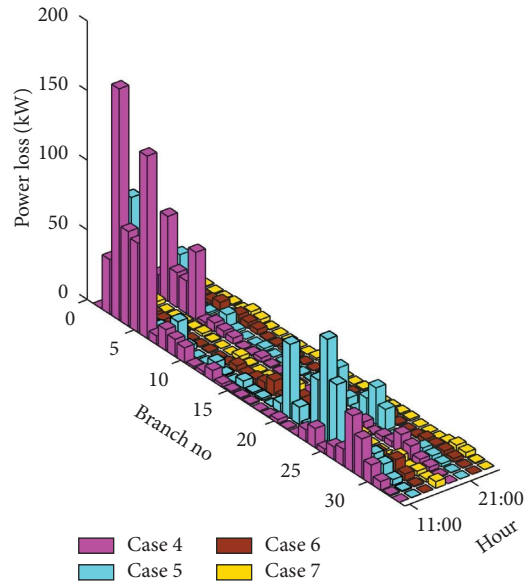

Figure 8: Power loss of each branch at 11:00 and 21:00.

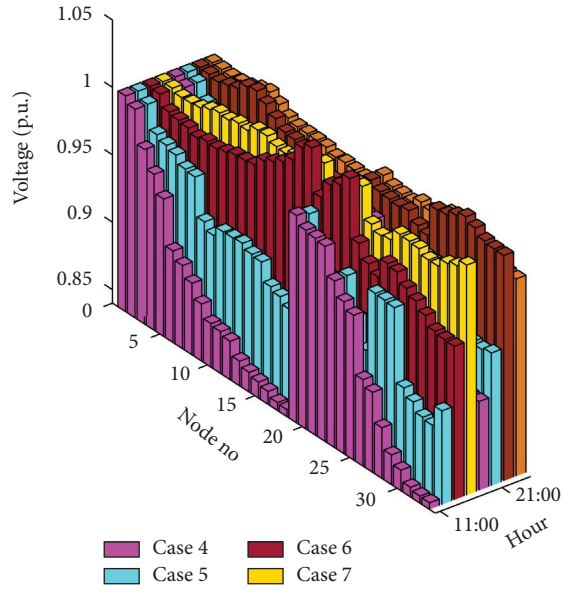

Figure 9: Voltage profile of each node at 11:00 and 21:00.

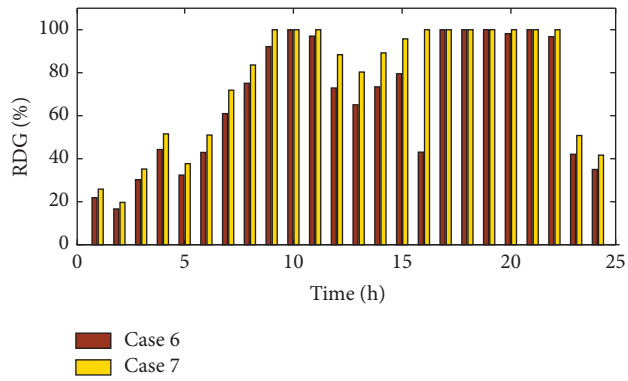

Fig 10: RDG utilization at of each time interval in case 6 and case 7.

Table 5: The open switches of four algorithms at each time interval.

Hour	open switches				
	HPSO	BPSO	BAS	GA	MFO
0	e18, e26, e15, e35, e13	e7, e14, e9, e32, e28	e3, e14, e11, e32, e28	e18, e26, e15, e35, e13	e18, e26, e15, e35, e13
1	e18, e26, e15, e35, e13	e7, e14, e9, e32, e28	e33, e14, e11, e32, e3	e18, e26, e15, e35, e13	e18, e26, e15, e35, e13
2	e18, e26, e15, e35, e13	e7, e14, e9, e32, e28	e33, e14, e10, e36, e3	e18, e26, e16, e11, e12	e18, e25, e16, e11, e12
3	e18, e26, e15, e35, e13	e7, e14, e9, e32, e28	e33, e13, e10, e17, e3	e18, e26, e16, e35, e13	e18, e25, e16, e35, e13
4	e18, e26, e15, e35, e13	e7, e14, e9, e32, e28	e33, e14, e11, e32, e4	e18, e26, e16, e35, e13	e18, e26, e16, e11, e12
5	e18, e26, e15, e35, e13	e7, e14, e9, e32, e28	e33, e13, e11, e17, e3	e18, e27, e16, e35, e13	e18, e26, e16, e35, e13
6	e18, e26, e15, e35, e13	e7, e14, e9, e32, e37	e33, e14, e11, e32, e3	e19, e26, e15, e21, e13	e19, e26, e15, e21, e13
7	e33, e26, e34, e11, e13	e7, e14, e9, e32, e28	e33, e14, e11, e16, e4	e33, e25, e15, e11, e13	e33, e26, e15, e11, e13
8	e33, e27, e34, e10, e14	e7, e14, e9, e32, e28	e33, e11, e21, e15, e4	e33, e27, e34, e10, e14	e33, e27, e34, e9, e13
9	e20, e28, e7, e9, e14	e7, e14, e9, e32, e28	e6, e34, e9, e14, e28	e20, e28, e7, e9, e14	e20, e28, e6, e9, e14
10	e19, e5, e34, e8, e14	e7, e14, e9, e32, e28	e6, e14, e10, e15, e28	e19, e5, e34, e8, e14	e19, e 5, e8, e9, e14
11	e7, e28, e8, e10, e14	e7, e14, e9, e32, e28	e5, e14, e10, e15, e28	e7, e28, e34, e8, e14	e7, e14, e9, e32, e28
12	e3, e28, e8, e9, e13	e7, e14, e9, e32, e37	e33, e9, e6, e14, e28	e7, e4, e8, e9, e14	e7, e4, e8, e10, e14
13	e7, e28, e8, e9, e14	e7, e14, e9, e32, e37	e5, e13, e9, e15, e28	e7, e28, e8, e10, e14	e7, e28, e8, e10, e14
14	e7, e28, e8, e10, e14	e7, e14, e9, e32, e28	e33, e34, e9, e14, e5	e7, e28, e8, e10, e14	e7, e28, e8, e10, e14
15	e6, e37, e15, e8, e 14	e7, e14, e9, e32, e28	e6, e34, e9, e14, e37	e6, e37, e15, e9, e 34	e6, e37, e15, e9, e 34
16	e20, e5, e15, e10, e 14	e7, e14, e9, e32, e37	e5, e13, e9 15, e28	e20, e5, e15, e9, e 14	e20, e5, e15, e10, e 14
17	e33, e4, e17, e11, e14	e7, e14, e9, e32, e28	e33, e14, e11, e17, e4	e33, e4, e32, e11, e14	e33, e4, e17, e11, e14
18	e33, e28, e32, e10, e14	e7, e14, e9, e32, e37	e33, e11, e6, e14, e28	e33, e28, e32, e10, e14	e33, e28, e32, e10, e14
19	e33, e3, e17, e35, e13	e7, e14, e9, e32, e37	e33, e13, e11, e36 , e4	e33, e3, e16, e35, e13	e33, e3, e17, e35, e13
20	e33, e4, e17, e11, e13	e7, e14, e9, e32, e28	e33, e14, e11, e36, e4	e33, e4, e17, e11, e13	e33, e4, e17, e11, e13
21	e33, e28, e17, e35, e13	e7, e14, e9, e32, e28	e33, e14, e11, e36, e3	e33, e28, e17, e35, e13	e33, e28, e17, e35, e13
22	e18, e26, e15, e35, e13	e7, e14, e9, e32, e37	e33, e13, e10, e36, e3	e18, e26, e15, e35, e13	e18, e26, e15, e35, e13
23	e18, e26, e15, e35, e13	e7, e14, e9, e32, e28	e33, e14, e11, e36, e3	e18, e2, e15, e35, e12	e18, e26, e15, e 35, e13

Table 6: Obtained results.

Items	*Total P_{loss}/MWh*	*RDG%*	*V_{min}/pu*
HPSO	1.2290	75.37%	0.9463
GA	1.2335	75.22%	0.9461
MFO	1.2302	75.28%	0.9463
BPSO	2.3031	50.98%	0.8848
BAS	1.3446	54.53%	0.9409

simultaneously combining network optimization with the integration of RDG are investigated in case 7. The obtained final opening switch combinations at 11:00 and 21:00 are [e7, e28, e8, e10, e14] and [e33, e28, e17, e35, e13], respectively. It provides a reduction to 63.2703kW at 11:00 and 28.3297kW at 21:00 of system power loss, which is significantly lower than that of other cases.

Fig 9 shows the voltage profile at two-time interval points. In case 4, voltage violations occur in most of the nodes which leads to an unsatisfactory low voltage profile. The network performance is improved by using network optimization and integration of RDGs simultaneously. It is observed that the system voltage volatility range is reduced in case 7. And the minimum voltage profile in cases 4-7 are 0.8449 p.u. for node 33 at 11:00, 0.8943 p.u. for node 32 at 11:00, 0.9539 p.u. for node 33 at 11:00, 0.9912 p.u. for node 24 at 11:00. The minimum voltage of ADN has raised dramatically with the network optimization and RDG integration.

As seen in Table 4, the absorption RDG power at two-time intervals by the system of case 6 are 5.2497 MW and 3.4541MW, while the optimization system of case 7 reaches 6.3646MW and 3.5698MW. It turns out that the absorption power of RDGs in case 6 is increased by 21.24% at 11:00 and

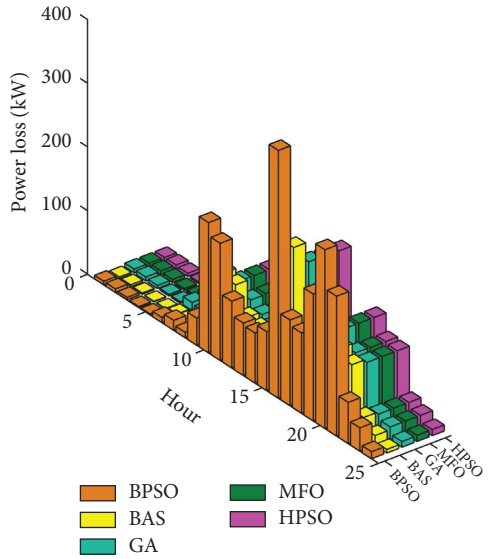

Figure 11: Comparison of power loss at each time interval.

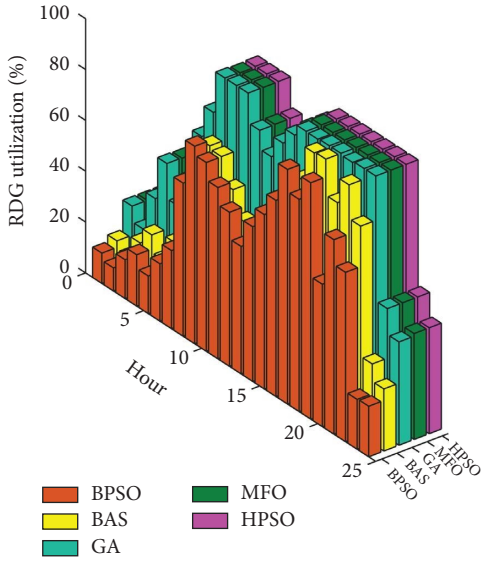

Figure 12: Comparison of RDG utilization at each time interval.

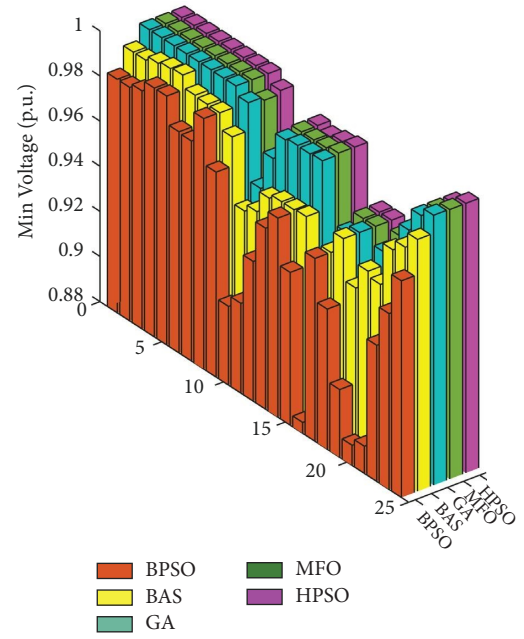

Figure 13: Comparison of minimum voltage at each time interval.

3.4% at 21:00 in case 6. The RDG utilization of a day in case 7 has increased by 15.48% and 3.24% compared to case 6. Moreover, Fig 10 compares the absorption RDG power over 24 hours for cases 6 and 7. The minimum RDG utilization in case 7 is 19.68% at 17:00, which is higher 16.64% in case 6. In both cases, the maximum difference of RDG utilization has reached to 56.94%. Thus, considering the time variations in load and RDG, the operational performance of the ADN would improve by using the proposed dynamic optimization model and the HPSO method.

4.1.3. Comparing the results of HPSO and Other Methods. As a comparison, the optimization problem of ADN considering time variation feature is also addressed by the methods of BPSO [19], BAS (beetle antennae search algorithm) [37], GA [43] and MFO [44].

Using all the methods, the list of final open switches for the best solutions during 24 hours are listed in Table 5. The

Table 7: The simulation results of 69-bus ADN in a day.

Items	*Total P_{loss}/MW*	*Total RDG/MW*	*V_{min}/pu*
Case 4	94.4404	0	0.4092
Case 5	1.8752	0	0.8079
Case 6	180.9674	83.5132	0.5476
Case 7	1.4379	123.6139	0.9203

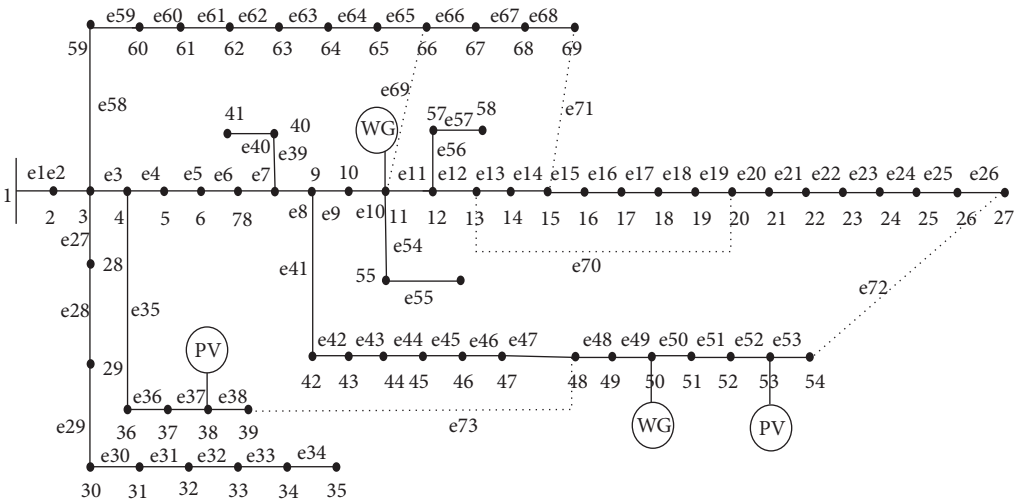

Figure 14: 69-bus ADN.

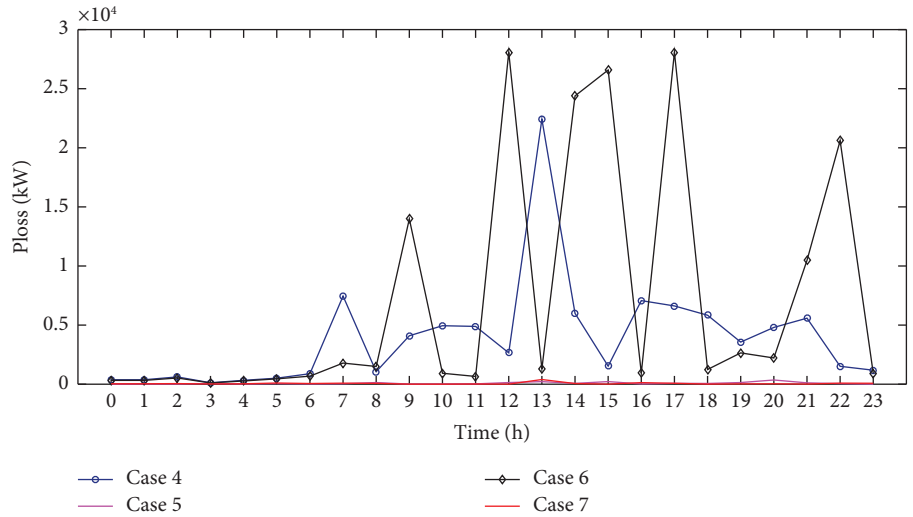

Figure 15: Power loss of 69-bus ADN during 24 hours.

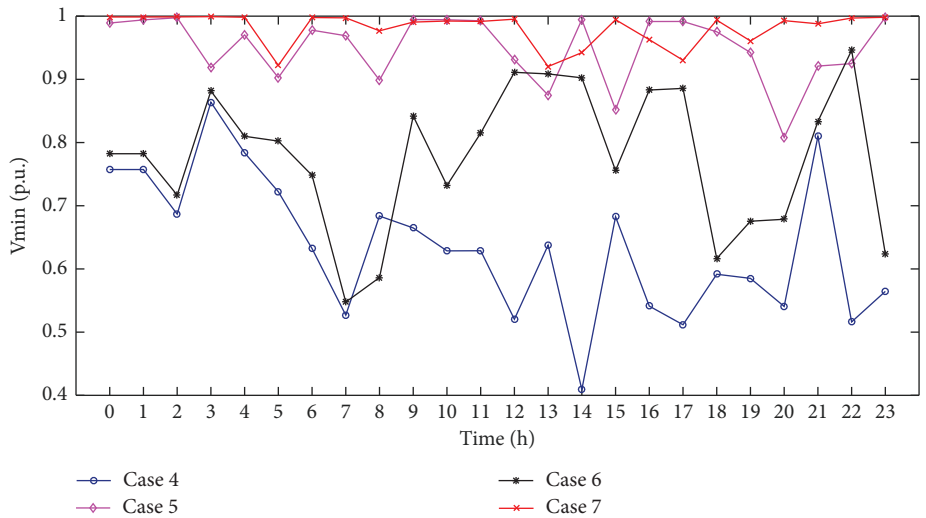

Figure 16: Voltage profiles of 69-bus ADN during 24 hours.

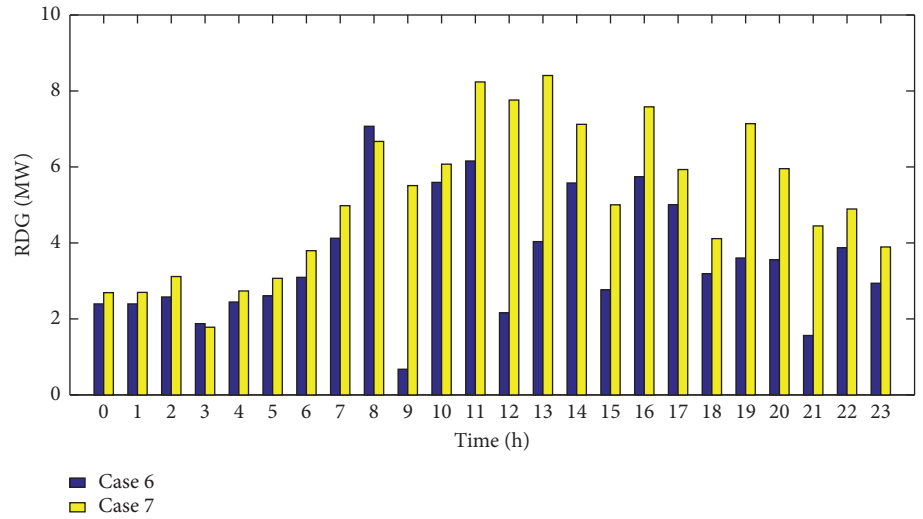

Figure 17: Absorbed RDG power of 69-bus ADN during 24 hours.

Table 8: Open switches of hourly optimization for 69-bus ADN.

Hour	Case 4	Case 5	Case 6	Case 7
0		e64, e14, e68, e44, e38		e4, e18, e13, e53, e47
1		e3, e18, e67, e50, e42		e4, e17, e14, e26, e47
2		e3, e18, e12, e47, e7		e4, e18, e13, e53, e47
3		e69, e19, e62, e50, e47		e4, e18, e13, e53, e47
4		e4, e16, e14, e53, e38		e4, e18, e13, e25, e47
5		e4, e17, e68, e52, e38		e4, e18, e13, e72, e47
6		e65, e17, e71, e52, e36		e4, e18, e13, e24, e47
7		e10, e15, e13, e12, e35		e4, e16, e13, e20, e41
8		e9, e15, e68, e20, e37		e7, e18, e13, e50, e47
9		e3, e16, e11, e13, e36		e3, e15, e5, e12, e45
10		e3, e17, e 68, e11, e4		e3, e17, e9, e12, e7
11	e69, e70, e71, e72, e73	e8, e70, e68, e11, e36	e69, e70, e71, e72, e73	e69, e13, e 67, e48, e7
12		e9, e70, e12, e16 , e36		e61, e16, e7, e12, e41
13		e9, e15, e13, e20, e36		e10, e15, e68, e11, e5
14		e3 e70, e 66, e11, e7		e3, e15, e71, e50, e41
15		e10, e15, e13, e23, e37		e69, e13, e5, e49, e35
16		e8, e16, e13, e11, e36		e65, e16, e14, e20, e47
17		e8, e15, e71, e11, e35		e3, e17, e68, e20, e7
18		e8, e17, e11, e13, e36		e60, e15, e9, e11, e36
19		e8, e15, e66, e12, e38		e3, e19, e68, e21, e5
20		e9, e15, e68, e22, e36		e65, e16, e68, e53, e7
21		e9, e18, e12, e14, e35		e4, e18, e68, e20, e36
22		e10, e15, e68, e25, e36		e4, e18, e13, e72, e47
23		e3, e19, e11, e26, e36		e4, e15, e68, e25, e47

crucial constraint for the radial structure is satisfied for each topology. According to the optimal topologies, Fig 11 shows the power loss, minimum voltage standard amplitude, and RDG utilization based on case 7 using HPSO, BPSO, BAS, GA and MFO for the ADN. The obtained results show that the indexes of the proposed HPSO are better than other methods for ADN optimization considering time variations in load and RDG over 24 hours.

The power loss of the 33-bus ADN after optimization during 24 hours is shown graphically in Fig 11. The maximum total power loss for the methods over 24 hours is 194.9442 kWh (HPSO), 389.0171 kWh (BPSO), 227.4633 kWh (BAS), 195.7518 kWh (GA), and 195.2001 kWh (MFO) at 15 p.m.

Fig 12 shows the RDG utilization after optimization at each time interval of a day. The results show that the minimum RDG utilization for each algorithm over 24 hours is 19.6811%, 9.0749%, 11.0089%, 19.6928%, and 19.6811%. The maximum RDG utilization for each algorithm over 24 hours is 100%, 92.9588%, 99.9970%, 99.9940%, and 100%. Moreover, the RDG utilization has reached 100% in eight-time intervals, which is obviously better than other methods.

The minimum voltage profiles of the ADN after optimization in a day are illustrated in Fig 13. The day minimum voltage amplitude of each algorithm is 0.9463 p.u., 0.8848 p.u., 0.9409p.u., 0.9461 p.u., and 0.9463 p.u. at 15 p.m. The minimum node voltage for a day is almost the same as that of

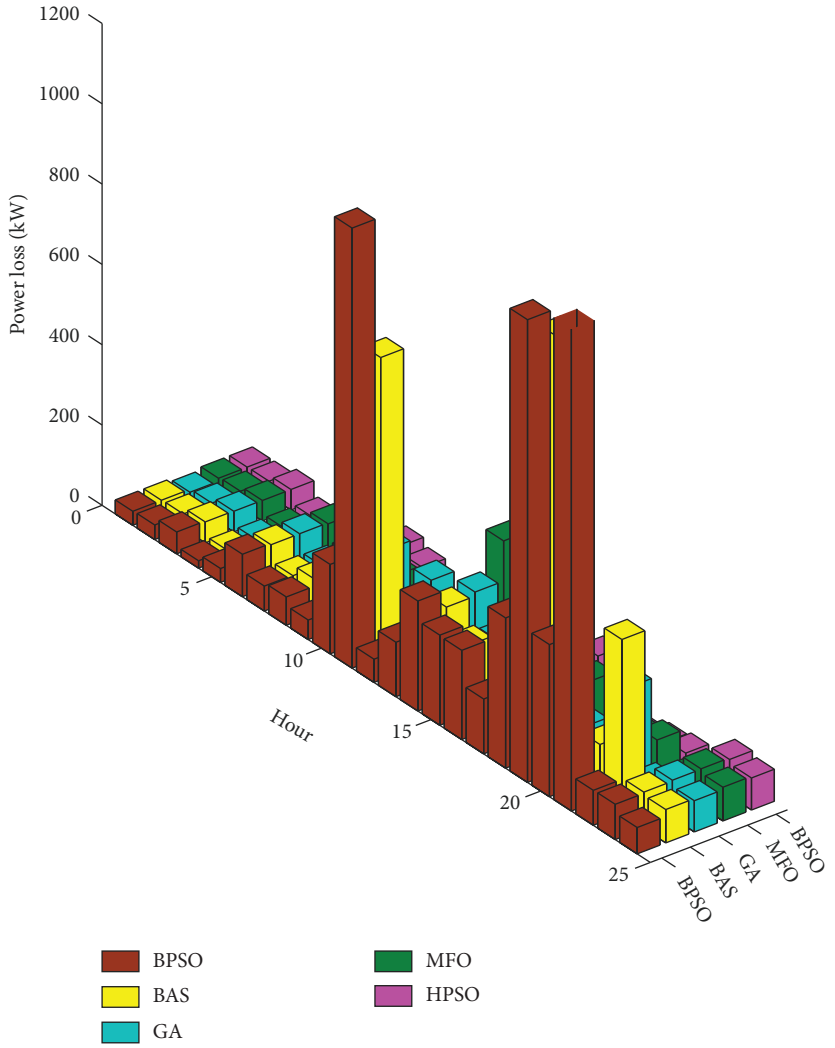

Figure 18: Comparison of power loss of 69-bus ADN.

MFO, but 0.21%, 0.57%, and 6.95% higher than GA, BAS, and BPSO.

Table 7 shows the total active power loss and RDG utilization in a day. The day power loss by the proposed HPSO is 1.2290MWh which is lower than 1.2302MWh (GA), 1.2335MWh (MFO), 1.3346MWh (BAS), and 2.3031MWh (BPSO). The RDG utilization for a day using HPSO, GA, MFO, BAS, and BPSO are 75.37%, 75.22%, 75.28%, 54.53%, and 50.98%, respectively. From all the results, we can see that the obtained results of HPSO algorithm are better to compare the GA, MFO, BAS, and BPSO. Thus, the proposed HPSO method is better in global optimization ability.

4.2. 69-bus ADN. The 69-bus ADN consists of 69 buses and 5 tie branches, as provided in Fig 14 [44]. The wind RDGs are connected to nodes 11 and 50. The PV RDGs are connected to nodes 38 and 53. The open switches in the initial network are e69, e70, e71, e72, and e73. The proposed method is applied to obtain the optimal reconfigure to enable RDG penetration. The hourly load demand for the system is obtained by using the method in [43].

For the sake of investigating the optimal problem of the ADN considering time variations in load and RDG, cases 4-7 will be implemented to the 69-bus ADN. Table 7 provides simulated results of the test active distribution network for 24 hours using the proposed method.

The original network considers the time-varying nature of load demand without the integration of RDGs and network optimization. From Table 7, we observe that the total daily active power loss of 94.4404MW for case 4. After network optimization, the total power loss has been reduced to 1.8752MW in case 5. To discuss the RDG effect, consider the integration of RDGs as case 6. The total power loss of the case is calculated as 169.0020MW. When both network optimization and RDG integration are considered, the daily power loss is minimized to 1.4379MW. Fig 15 shows active power loss for the four cases during 24 hours. In all hours, the power loss has been reduced greatly using network optimization and integration of RDGs in case 7.

The voltage profiles of the cases during 24 hours have been illustrated in Fig 16. The hourly minimum voltages in cases are 0.4092p.u. at 15:00, 0.8079 p.u. at 21:00,

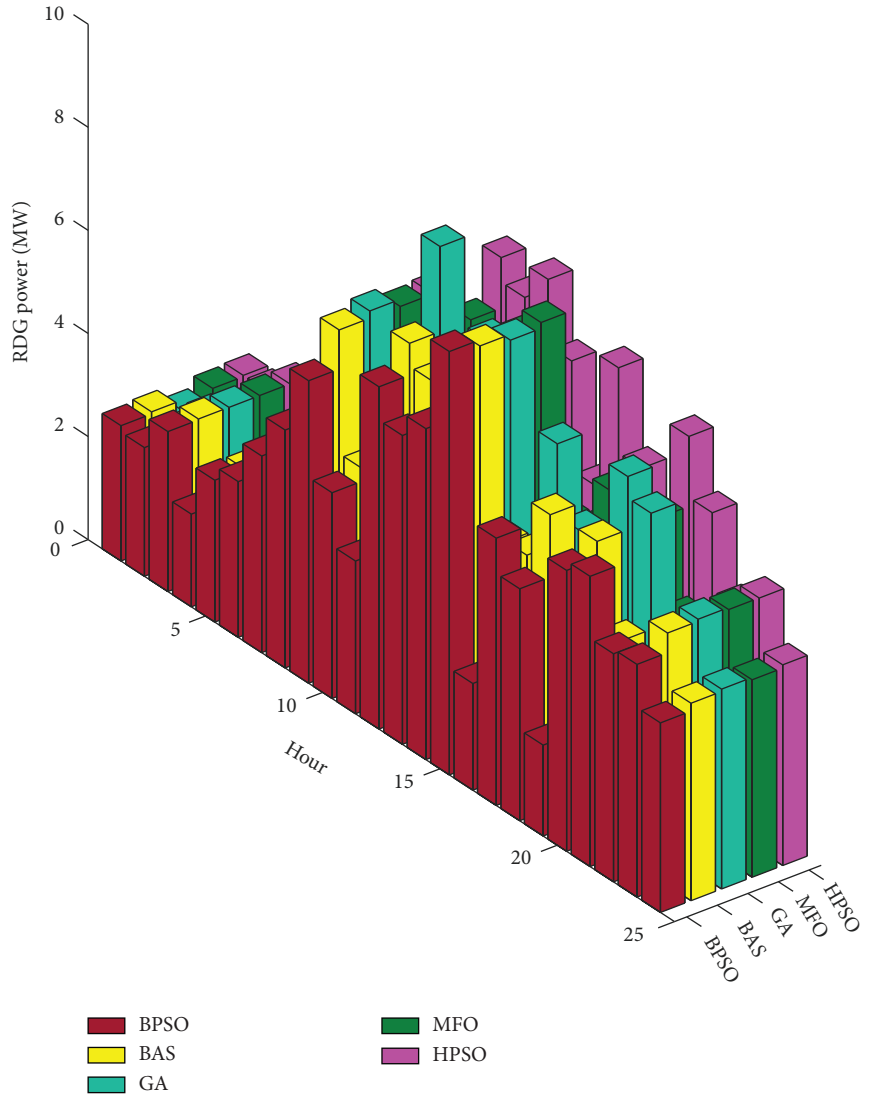

Figure19: Comparison of RDG utilization of 69-bus ADN.

0.5476 p.u. at 8:00, and 0.9203 p.u. at 14:00, respectively. It is observed that the minimum voltage profile for cases 4-6 is lower than the lower voltage limit 0.9p.u. The network optimization based on time variation of RDGs and load demand brings much less voltage fluctuations with respect to case 7 than case 5 and case 6 because the scheme considers the network optimization and integration of RDGs.

Fig 17 also compares the absorbed RDG power by the system at each interval before and after network optimization (case 6 and case 7). We observe that the total absorbed RDG power after optimization for a day is 123.6139MW, which has increased by 45.40% before the system. The RDG utilization has been improved from 52.93% to 76.96% after optimization. With the expansion of network structure, the proposed method is more effective for improving the operation indices of the ADN.

Table 8 shows the open switches of the hourly optimization solution for the cases. The application of network optimization to the ADN has permitted to achieve a better operational conditions. As an example, the topological structure [e7, e18, e13, e50, e47] is optimal for the hour 8:00 of the day in case 7. It ensures a reduction of 93.37%, 49.97%, and 95.32% of power loss with other cases. In addition, The voltage profile is increased by 42.87%, 8.68% and 66.58% for case 4, case 5, and case 6, respectively. And the absorbed RDG power of case 7 is improved to 6.6721MW which is higher than 4.8958MW of case 6. These results show that the proposed model and method yield acceptable results in terms of power loss reduction, voltage improvement, and RDG utilization for both test systems under time variations of load demand and RDG. This demonstrates the ability of the proposed approach to find the optimal network topology along with absorbed RDG power and load demand for the ADN considering time characteristics.

To further illustrate the superiority of the HPSO, we compared and analyzed the 24 hours simulated results of case 7 by methods of HPSO, BPSO, BAS, GA, and MFO. Fig 18–20 show the comparison of the proposed HPSO and the conventional approaches BPSO, BAS, GA, and

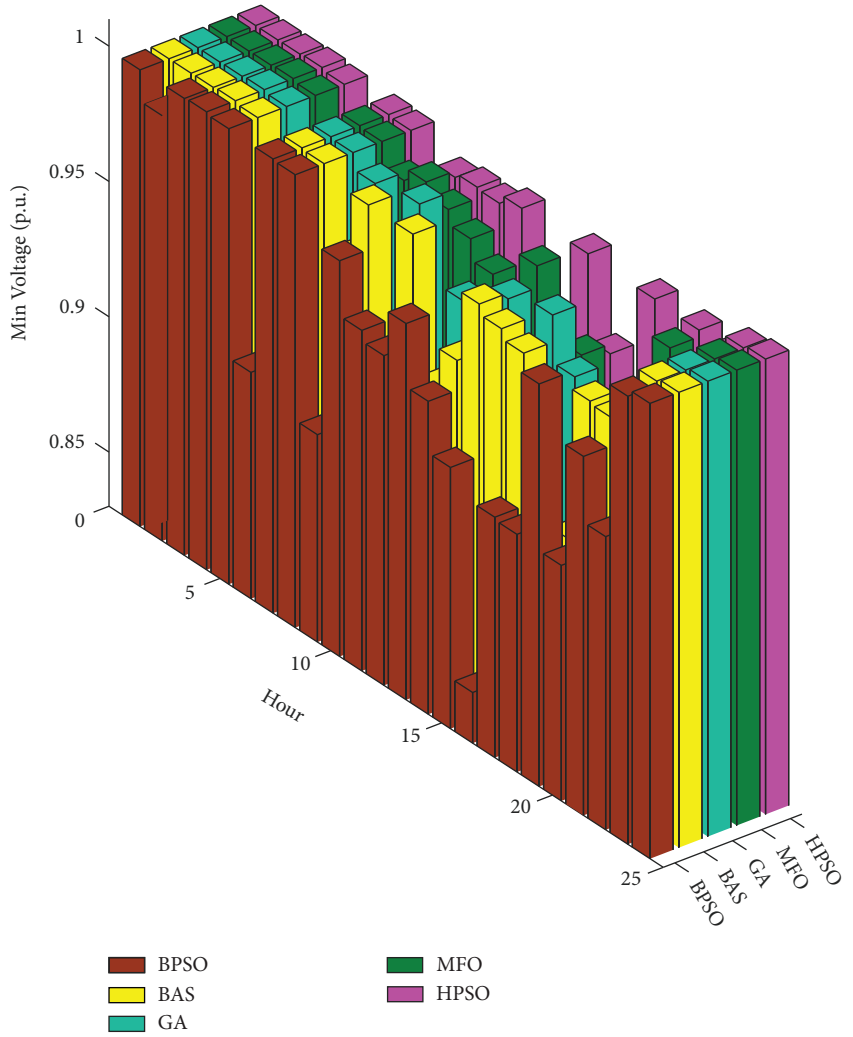

Figure 20: Comparison of minimum voltage of 69-bus ADN.

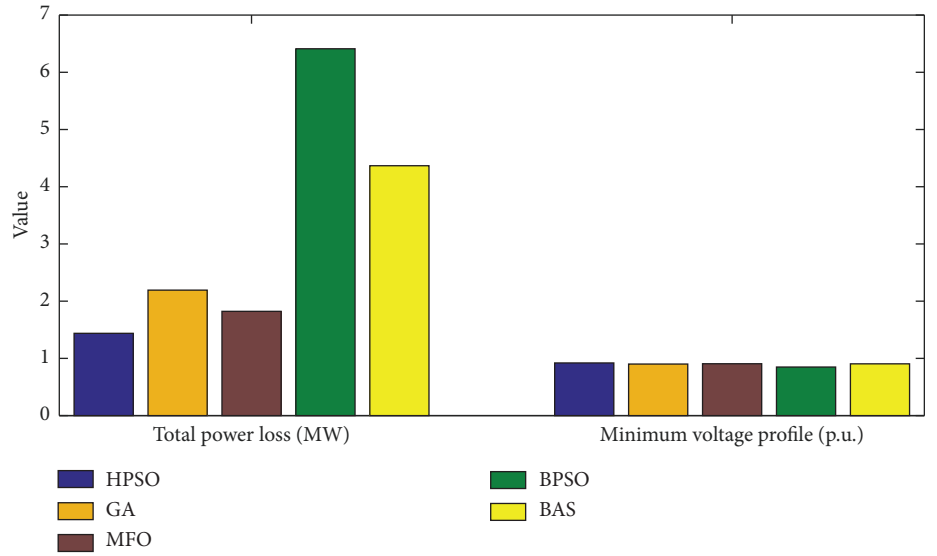

Figure 21: Comparison total power loss and minimum voltage profile for all the methods in a day.

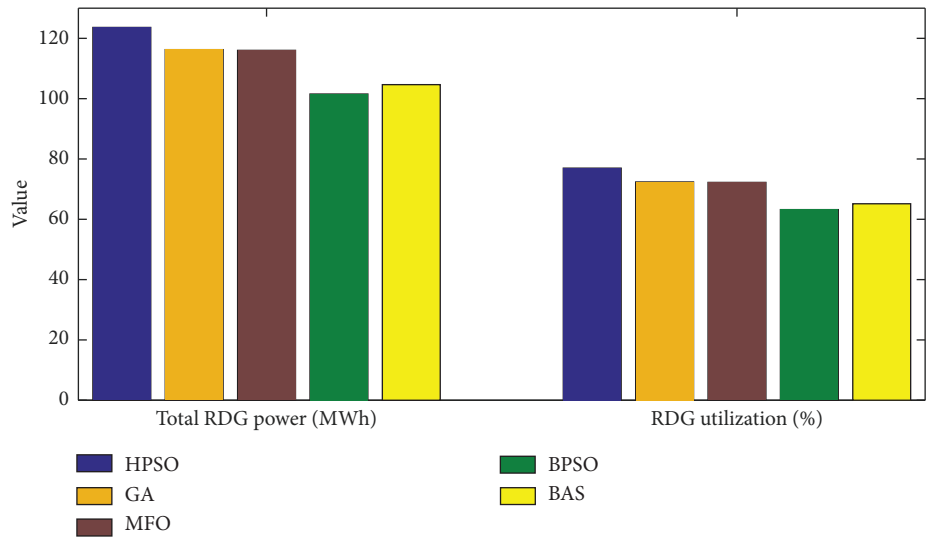

Figure 22: Comparison RDG power and RDG utilization for all the methods in a day.

MFO. And the comparison of the simulation results in a day is also shown in Fig 21–22. We can clearly the minimum voltage profiles in a day are 0.9203 p.u. for HPSO, 0.8487 p.u. for BPSO, 0.9048 p.u. for BAS, 0.9009 p.u. for GA, 0.9066 p.u. for MFO, respectively. From Fig 18, the total active power loss of a day 1.4379 MWh by HPSO, which is less 77.57%, 67.07%, 34.34%, and 21.09% than BPSO, BAS, GA, and MFO. The day RDG utilization with a penetration rate of 76.96% is the highest among all the methods. Thus, considering the overall operation economy in terms of power loss, voltage quality, and RDG utilization, the proposed HPSO is superior to the other methods.

5. Conclusions

In this paper, a successful multi-period optimization strategy of the ADN considering time variations in load demand and RDG has been presented. The objective function of the dynamic optimization model includes the power loss and the RDG utilization for a given time to ensure optimal operation of the ADN. Additionally, the average weigh factors approach is used to balance the relationship of the objectives in multi-period optimization model. Furthermore, the proposed HPSO algorithm and the optimization model are combined to determine the optimal topology and RDG resource allocation scheme for each time interval in the ADN.

The optimization strategy considers different possibilities of network optimization, time variations of load demand and RDG. The proposed optimization model and HPSO method test on the 33-bus and 69-bus ADNs to verify the effectiveness. The simulation results show that the proposed strategy obtains reasonable and high-quality schedules for switching and the active power values of RDGs in multi-period optimization objective frameworks. Additionally, considering the network optimization helps significantly increase RDG utilization and improve the voltage profile in a day. Case studies are conducted on 33-bus and 69-bus ADNs under different operating conditions. Simulation results show that the proposed strategy can find the corresponding optimal solution in each time interval. Thus, the performance of the ADN can be improved by integrating RDG and network optimization. Moreover, the superiority of the proposed optimization algorithm considering time variations of load and RDG is proved by comparing conventional methods. This paper presents a management strategy for ADN considering time variations in load and RDG, which is an important requirement to mostly explore the benefits without extra investment costs or system risks. However, the switches in the optimization process would be changed constantly according to time intervals. The influence of frequent switch action is ignored in this paper. The author suggestion for future study would be to modify the method according to the switch constraint. [21, 45].

Abbreviations

k:	Label of sub time interval
i, j:	Node label
m:	Particle label
l:	Branch label
h:	RDG label
N_l:	Number of branches
N_G:	Number of RDGs
N_H:	Number of time intervals
n:	Number of loops
max:	Maximum upper limit
min:	Minimum lower limit
P_R^k:	Residential power load
P_I^k:	Industrial power load
P_C^k:	Commercial power load
P_r:	Rated power of wind RDG
P_w^k:	Actual output power of wind RDG

v_{in}^k: Cut in wind speed
v_{out}^k: Cut out wind speed
v_r^k: Rated wind speed
$\Gamma(\cdot)$: Gamma function
r: Solar irradiance
α, β: Shape parameters of beta distribution
P_{Vw}^k: Actual power output of photovoltaic RDG
E_p: Maximum power of photovoltaic RDG
A: Total area
η_{pv}: Weighted photoelectric conversion efficiency
φ: Power factor angle
P_l^k: Active power of lth branch
Q_l^k: Reactive power of lth branch
r_l^k: Branch resistance
U^k: Node voltage amplitude
δ_h: Connection status between RDG and network
z_l^k: Switch status
$F_{\text{RDG\%}}$: RDG utilization
N_G: RDG number
δ_i: Binary variable
P_{RDG}^k and Q_{RDG}^k: Actual active and reactive power of RDG
$P_{\hat{s}}^k$ and $Q_{\hat{s}}^k$: Injected active and reactive power
P_L^k and Q_L^k: Active and reactive power of load
g_l^k: Conductance value
b_l^k: Susceptance value
θ_l^k: Phase angle
z_l^k: Switch status
T_G^k: Network topology
T_{Gr}: Topology set
S_l^k: Apparent power flow
X_d: Particle vector
p_{md}^k, p_{gd}^k: Best particle position and the globally best particle position
σ_1, σ_2: Weight coefficient of optimization indices
λ^k: Control parameter
RDG: Renewable distributed generation
ADN: Active distribution network
GA: Genetic algorithm
I-DBEA: Improved decomposition based evolutionary algorithm
PSO: Particle swarm optimization
PDF: Probability density function
HPSO: Hybrid particle swarm optimization
MFO: Moth-flame optimization
PV: Photovoltaic
BAS: Beetle antennae search algorithm.

Data Availability

The data used to support the findings of this study are included within the article.

Conflicts of Interest

The authors declare that there are no conflicts of interest regarding the publication of this article.

Authors' Contributions

Juan Wen and Xing Qu designed and performed the study, acquired and analyzed data, and drafted the manuscript. Xing Qu and Siyu Lin reviewed the study design, helped analyze the data, and revised the manuscript text. Lin Ding and Lin Jiang helped analyze the data. All authors read and approved the final manuscript.

Acknowledgments

The authors would like to acknowledge the many helpful suggestions of the anonymous reviewers and the editor, which have improved the content and the presentation of this paper. This work was supported by National Natural Science Foundation of China (62003157), Technology Planning Project of Hunan Province (2020JJ5498), Research Foundation of Education Bureau of Hunan Province (21B0434), and Planning Project of University of South China (190XQD128). Also, we thank the 2022 7th Asia Conference on Power and Electrical Engineering where the main idea of this paper was presented.

References

[1] A. Demirbaş, "Global renewable energy resources," *Energy Sources, Part A: Recovery, Utilization, and Environmental Effects*, vol. 28, no. 8, pp. 779–792, 2006.

[2] F. Blaabjerg and K. Ma, "Future on power electronics for wind turbine systems," *IEEE J. Emerg. Sel. Topics Power Electron.*vol. 1, no. 3, pp. 139–152, 2013.

[3] A. M. Foley, B. Ó Gallachóir, E. J. McKeogh, D. Milborrow, and P. G. Leahy, "Addressing the technical and market challenges to high wind power integration in Ireland," *Renewable and Sustainable Energy Reviews*, vol. 19, pp. 692–703, 2013.

[4] Irena, *Global Energy Transformation: A Roadmap to 2050*, IRENA, Abu Dhabi, United Arab Emirates, 2019.

[5] W. Jing, C. H. Lai, W. S. H. Wong, and M. D. Wong, "A comprehensive study of battery-supercapacitor hybrid energy storage system for standalone PV power system in rural electrification," *Applied Energy*, vol. 224, pp. 340–356, 2018.

[6] J. Moccia, A. Arapogianni, J. Wilkes, C. Kjaer, R. Gruet, and S. Azau, "Brussels, Belgium," in *Pure Power: Wind Energy Targets for 2020 and 2030*Tech. Rep, 2011.

[7] J. Liu and H.-D. Chiang, "Maximizing available delivery capability of unbalanced distribution networks for high penetration of distributed generators," *IEEE Transactions on Power Delivery*, vol. 32, no. 3, pp. 1196–1202, 2017.

[8] H. Sekhavatmanesh and R. Cherkaoui, "A novel decomposition solution approach for the restoration problem in distribution networks," *IEEE Transactions on Power Systems*, vol. 35, no. 5, pp. 3810–3824, 2020.

[9] X. Zhao, X. Shen, Q. Guo, H. Sun, and S. S. Oren, "A stochastic distribution system planning method considering regulation services and energy storage degradation," *Applied Energy*, vol. 277, pp. 1–13, 2020.

[10] A. Noori, Y. Zhang, N. Nouri, and M. Hajivand, "Multi-objective optimal placement and sizing of distribution static compensator in radial distribution networks with variable residential commercial and industrial demands considering reliability," *IEEE Access*, vol. 9, pp. 46911–46926, 2021.

[11] M. E. Baran and F. F. Wu, "Network reconfiguration in distribution systems for loss reduction and load balancing," *IEEE Transactions on Power Delivery*, vol. 4, no. 2, pp. 1401–1407, 1989.

[12] C. Joon-Ho and K. Jae-Chul, "Advanced voltage regulation method of power distribution systems interconnected with dispersed storage and generation systems," *IEEE Transactions on Power Delivery*, vol. 16, no. 2, pp. 329–334, 2001.

[13] A. Merlin and H. Back, "Search for a minimal-loss operating spanning tree configuration in an urban power distribution system," in *Proc. 5th Power Syst. Comput. Conf*pp. 1–18, Cambridge, U.K, 1975.

[14] M. W. Siti, D. V. Nicolae, A. A. Jimoh, and A. Ukil, "Reconfiguration and load balancing in the LV and MV distribution networks for optimal performance," *IEEE Transactions on Power Delivery*, vol. 22, no. 4, pp. 2534–2540, 2007.

[15] A. Mendes, N. Boland, P. Guiney, and C. Riveros, "Switch and tap-changer reconfiguration of distribution networks using evolutionary algorithms," *IEEE Transactions on Power Systems*, vol. 28, no. 1, pp. 85–92, 2013.

[16] M. J. H. Moghaddam, A. Kalam, J. Shi, S. A. Nowdeh, F. H. Gandoman, and A Ahmadi, "A new model for reconfiguration and distributed generation allocation in distribution network considering power quality indices and network losses," *IEEE Systems Journal*, vol. 14, no. 3, pp. 3530–3538, 2020.

[17] Z. Liu, Y. Liu, G. Qu, X. Wang, and X. Wang, "Intra-day dynamic network reconfiguration based on probability analysis considering the deployment of remote control switches," *IEEE Access*, vol. 7, pp. 145272–145281, 2019.

[18] A. Ali, M. U Keerio, and J. A Laghari, "Optimal site and size of distributed generation allocation in radial distribution network using multi-objective optimization," *Journal of Modern Power Systems and Clean Energy*, vol. 9, no. 2, pp. 404–415, 2021.

[19] T. T. Nguyen and T. T. Nguyen, "An improved cuckoo search algorithm for the problem of electric distribution network reconfiguration," *Applied Soft Computing*, vol. 84, p. 105720, 2019.

[20] H. S. Ramadan, A. F. Bendary, and S. Nagy, "Particle swarm optimization algorithm for capacitor allocation problem in distribution systems with wind turbine generators," *International Journal of Electrical Power & Energy Systems*, vol. 84, pp. 143–152, 2017.

[21] G. S. Chawda, A. G. Shaik, O. P. Mahela, S. Padmanaban, and J. B. Holm-Nielsen, "Comprehensive review of distributed FACTS control algorithms for power quality enhancement in utility grid with renewable energy penetration," *IEEE Access*, vol. 8, pp. 107614–107634, 2020.

[22] J. Shukla, B. Das, and V. Pant, "Stability constrained optimal distribution system reconfiguration considering uncertainties in correlated loads and distributed generations," *International Journal of Electrical Power & Energy Systems*, vol. 99, no. 1, pp. 121–133, 2018.

[23] Y. K. Wu, C. Y. Lee, L. C. Liu, and S. H. Tsai, "Study of reconfiguration for the distribution system with distributed generators," *IEEE Transactions on Power Delivery*, vol. 25, no. 3, pp. 1678–1685, 2010.

[24] A. Mohamed Imran, M. Kowsalya, and D. Kothari, "A novel integration technique for optimal network reconfiguration and distributed generation placement in power distribution networks," *International Journal of Electrical Power & Energy Systems*, vol. 63, pp. 461–472, 2014.

[25] M. A. Muhammad, H. Mokhlis, K. Naidu, and A. A. M. Othman, "Distribution network planning enhancement via network reconfiguration and DG integration using dataset approach and water cycle algorithm," *J. Mod. Power Syst. Cle.*vol. 8, no. 1, pp. 86–93, 2020.

[26] M. Falahi, S. Lotfifard, M. Ehsani, and K. Butler-Purry, "Dynamic model predictive-based energy management of DG integrated distribution systems," *IEEE Transactions on Power Delivery*, vol. 28, no. 4, pp. 2217–2227, 2013.

[27] A. Alonso-Travesset, H. Martín, S. Coronas, and J. de la Hoz, "Optimization models under uncertainty in distributed generation systems: a review," *Energies*, vol. 15, no. 5, pp. 1932–1940, 2022.

[28] Y. Gao, W. Wang, J. Shi, and N. Yu, "Batch-Constrained reinforcement learning for dynamic distribution network reconfiguration," *IEEE Transactions on Smart Grid*, vol. 11, no. 6, pp. 5357–5369, 2020.

[29] M. Rahmani-Andebili and M. Fotuhi-Firuzabad, "An adaptive approach for PEVs charging management and reconfiguration of electrical distribution system penetrated by renewables," *IEEE Transactions on Industrial Informatics*, vol. 14, no. 5, pp. 2001–2010, 2018.

[30] J. Jithendranath and D. Das, "Stochastic planning of islanded microgrids with uncertain multi-energy demands and renewable generations," *IET Renewable Power Generation*, vol. 14, no. 19, pp. 4179–4192, 2020.

[31] Z. Li, S. Jazebi, and F. De Leon, "Determination of the optimal switching frequency for distribution system reconfiguration," *IEEE Transactions on Power Delivery*, vol. 32, no. 4, pp. 2060–2069, 2017.

[32] R. Ebrahimi, M. Ehsan, and H. Nouri, "'A profit-centric strategy for distributed generation planning considering time varying voltage dependent load demand," *International Journal of Electrical Power & Energy Systems*, vol. 44, no. 1, pp. 168–178, 2013.

[33] F. Ding and K. A. Loparo, "Feeder reconfiguration for unbalanced distribution systems with distributed generation: a hierarchical decentralized approach," *IEEE Transactions on Power Systems*, vol. 31, no. 2, pp. 1633–1642, 2016.

[34] H. Wu, P. Dong, and M. Liu, "Distribution network reconfiguration for loss reduction and voltage stability with random fuzzy uncertainties of renewable energy generation and load," *IEEE Transactions on Industrial Informatics*, vol. 16, no. 9, pp. 5655–5666, 2020.

[35] A. Ahmed, M. F. Nadeem, I. A. Sajjad, R. Bo, I. A. Khan, and A. Raza, "'Probabilistic generation model for optimal allocation of wind DG in distribution systems with time varying load models," *Sustainable Energy, Grids and Networks*, vol. 22, pp. 1–12, 2020.

[36] D. Q. Hung, N. Mithulananthan, and K. Y. Lee, "Determining PV penetration for distribution systems with time-varying load models," *IEEE Transactions on Power Systems*, vol. 29, no. 6, pp. 3048–3057, 2014.

[37] S. Cheng and Z. Li, "'Multi-objective network reconfiguration considering V2G of electric vehicles in distribution system with renewable energy," *Energy Procedia*, vol. 158, pp. 278–283, 2019.

[38] J. Wang, W. Wang, Z. Yuan, H. Wang, and J. Wu, "A chaos disturbed beetle antennae search algorithm for a multi-objective distribution network reconfiguration considering the variation of load and DG," *IEEE Access*, vol. 8, pp. 97392–97407, 2020.

[39] J. Wen, X. Qu, Y. H. Huang, and S. Y. Lin, "A reconfiguration method of distribution network considering time variations

for load and renewable distributed generation," in *Proceedings of the 2022 7th Asia Conference on Power and Electrical Engineering*, pp. 544–549, Hangzhou, China, April 2022.

[40] W. ur Rehman, M. F. N. Khan, I. A. Sajjad, and M. Umar Afzaal, "Probabilistic generation model for grid connected wind DG," *Journal of Renewable and Sustainable Energy*, vol. 11, no. 4, pp. 045301–045312, 2019.

[41] Q. Chen, W. Wang, H. Wang, J. Wu, X. Li, and J. Lan, "A social beetle swarm algorithm based on grey target decision-making for a multiobjective distribution network reconfiguration considering partition of time intervals," *IEEE Access*, vol. 8, pp. 204987–205013, 2020.

[42] D. Q. Hung, N. Mithulananthan, and R. C. Bansal, "Analytical expressions for DG allocation in primary distribution networks," *IEEE Transactions on Energy Conversion*, vol. 25, no. 3, pp. 814–820, 2010.

[43] J. Sun, W. Fang, X. Wu, V. Palade, and W. Xu, "Quantum-behaved particle swarm optimization: analysis of individual particle behavior and parameter selection," *Evolutionary Computation*, vol. 20, no. 3, pp. 349–393, 2012.

[44] A. A. Hassan, F. H. Fahmy, A. E.-S. A. Nafeh, and M. A. Abu-elmagd, "Genetic single objective optimisation for sizing and allocation of renewable DG systems," *International Journal of Sustainable Energy*, vol. 36, no. 6, pp. 545–562, 2017.

[45] A. Jafar-Nowdeh, M. Babanezhad, S. Arabi-Nowdeh, A. Naderipour, and V. K. Ramachandaramurthy, "Meta-heuristic matrix moth-flame algorithm for optimal reconfiguration of distribution networks and placement of solar and wind renewable sources considering reliability," *Environmental Technology & Innovation*, vol. 20, pp. 101–118, 2020.